Cytidine- and guanosine-based nucleotide–lipids

Bruno Alies, Mohamed Ouelhazi, Amit Patwa, Julien Verget, Laurence Navailles, Valérie Desvergnes, Philippe Barthélémy

Cytidine- and guanosine-based nucleotide-lipids

Bruno Alies,[a] Mohamed A. Ouelhazi ,[a] Amit Patwa,[a,b] Julien Verget,[a] Laurence Navailles,[c] Valérie Desvergnes,[a] and Philippe Barthélémy[a]

Hybrid nucleotide-lipids composed of a lipid covalently attached to purine and pyrimidine nucleobases exhibit supramolecular properties. The novel cytidine and guanosine derivatives are promising bioinspired materials, which can act as supramolecular gelators depending on both the nucleobase and the presence of salts. These supramolecular properties are of broad interest for biomedical applications.

Introduction

Supramolecular materials derived from biological structures such as peptides,[1,2] carbohydrates,[3] or nucleosides[4] are attractive for various applications,[5,6] including green chemistry,[7,8] materials science, drug delivery,[9,10] medicinal chemistry,[11,12,13] tissue engineering, or regenerative medicine.[14] Nucleolipids,[15,16,17] which are biocompatible structures composed of a lipid covalently attached to a nucleotide, are desirable candidates for the implementation of supramolecular biomaterials as they easily engage non-covalent interactions.[18,19] Nucleotides-based lipids, in particular, are unique in that they have multiple possibilities for non-covalent interactions depending on the nature of the bases and can self-associate into stable different type of self-assembly, such as ribbons, bilayers, fibers etc. In previous studies, we reported the self-assembly properties of several nucleotide lipids (NLs) featuring 3'-monophosphate thymidine or adenosine head groups covalently attached to 1,2-dipalmitoyl-*sn*-glycerol.[20,21,22] Interestingly, biocompatible hydrogels, resulting from the self-assembly of thymidine-3'-(1,2-dipalmitoyl-*sn*-glycero-3-phosphate) (diC16-3'-dT) salts, were found to be effective soft materials for *in vivo* injection and implantation.[23]

The modulation of the polar head structure, in particular the nature of the base could influence the aggregation properties of the NLs. Therefore, we elected to design NLs with a double dipalmitoyl glycerol phosphate linked to the 3'-secondary hydroxyl of the four natural nucleosides. Indeed, the diverse hydrogen bond donor-acceptor sites in all four nucleobases (A: Adenine, T: Thymine C: Cytosine, and G: Guanine) are prone to form self-base pairing interactions that stabilize supramolecular self-assemblies.[24,25] It is therefore valuable to explore the self-assembly properties of A, C, T and G based nucleotide-lipids as supramolecular building blocks. Specifically, we report the synthesis and the physicochemical studies of a series of nucleoside-3'-monophosphate NLs featuring palmitic double chains and A, T, C, G nucleobases. Several examples of nucleoside-based amphiphiles have been reported,[26,27,28] however to the best of our knowledge, there are no previous examples of Cytosine and Guanosine nucleoside-3'-monophosphate amphiphiles.

Results and discussion

In this study, we prepared four purine and pyrimidine nucleotide-lipids *via* a phosphoramidite strategy. The supramolecular assemblies obtained with A, T, C, G nucleotide lipids either in the absence or presence of sodium chloride are reported (Fig. 1). Depending on both the conditions and the nature of the base the stabilisation of supramolecular hydrogels was observed. Likewise, as a proof of concept, *in vitro* drug release experiments show that a controlled delivery of a drug can be obtained thanks to the structure of the nucleolipid based gels.

Several strategies have been used to synthesize nucleotide lipids, including coupling reactions of monoalkyl phosphate with nucleoside and enzyme catalysis,[29] or *via* phosphoramidite synthetic pathway. The novel NLs, diC16-3'-dG **1a** and diC16-3'-dC **1b**, were synthesized using a similar approach to that used for the synthesis of diC16-3'-LNA-A[30] (see ESI, Scheme **S1**). This approach uses standard procedures, routinely adopted in oligonucleotide synthesis via phosphoramidite chemistry in the solid phase and adapted to solution. Briefly, commercially available isobutyryl protected guanosine phosphoramidite **2a** (isobutyryl-dG-CE phosphoramidite, see SI, Scheme **S1**) and acetyl protected cytosine phosphoramidite **2b** (Ac-dC-CE phosphoramidite, see SI, Scheme **S1**) were deprotected with methylamine solution in THF to achieve dG-CE phosphoramidite **3a** and dC-CE phosphoramidite **3b**, respectively. These phosphoramidites (**3a** and **3b**) were coupled with 1,2-dipalmitoyl-*sn*-glycerol in the presence of a tetrazole solution in acetonitrile (weakly acidic condition) to provide intermediate coupling product. The resulting phosphite intermediates were oxidized, with iodine solution in THF/pyridine/water mixture, to obtain cyanoethyl protected phosphate intermediate. After deprotection of the dimethoxytrityl (5'-DMTr) group under acidic conditions (trichloroacetic acid in DCM), the removal of the cyanoethyl chain was achieved under basic conditions (triethylamine) to

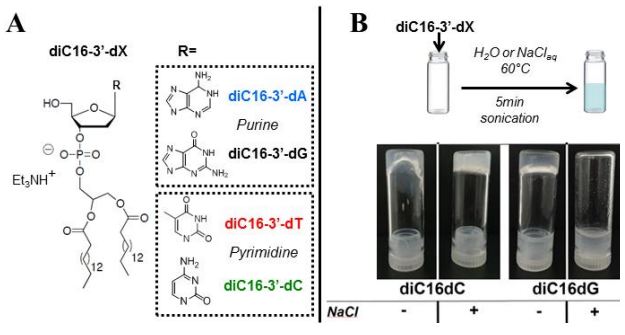

Fig. 1. A) Chemical structure of the nucleotide-lipid (NLs). B) Nucleotide lipid derivatives were incubated either in the absence or presence of sodium chloride. The novel C and G nucleotide lipid aqueous suspensions exhibit different macroscopic behaviors, the cytosine NL stabilizes hydrogels in the presence or NaCl, whereas the guanosine derivative forms a gel in the absence of NaCl.

yield diC16-3'-dG **1a** and diC16-3'-dC **1b** as their triethylammonium salts (for detailed synthetic procedure, see SI, Scheme **S1**). The NLs featuring thymidine (diC16-3'-dT **1c**)[31] and adenosinne (diC16-3'-dA **1d**),[32] were synthesized according to the literature procedure.

Spectroscopy studies

In order to study the inter-nucleobase interactions in the NLs self-assemblies UV-visible and Circular Dichroism experiments were performed. Figure 2 show the UV spectra of each NLs in aqueous (dashed line) or NaCl solution (dotted line) with their correspondent deoxynucleosides (solid line). It is well known that UV spectra of aromatic rings are sensitive to π-π interaction, when two or more rings are mutually close they give rise to hypochromic effect. A decrease of about 20 % in the absorbance values was observed for diC16-3'-dA, diC16-3'-dT and diC16-3'-dG compared with deoxyadenosine, thymidine and deoxyguanosine, respectively. In the case of diC16-3'-dC, no significant decrease in absorbance and slight bathochromic shift (5 nm) were observed compared to deoxycytidine. In order to get further structural information, circular dichroism (CD) of NLs and deoxynucleosides was also investigated (Fig. 2, right scale). Compared to deoxyadenosine (solid line), the CD spectra of diC16-3'-dA exhibited more pronounced peaks at 225 and 280 nm and the appearance of a band at 240 nm. With diC16-3'-dT, the band at 270nm is similar to thymidine. Preparation in NaCl (red dotted line) intensified the band. DiC16-3'-dG exhibited the appearance of two new peaks, a positive band at 240 nm and a negative band at 260 nm in addition to the peak at 225 nm observed in both CD spectra. With purine NLs (diC16-3'-dA & diC16-3'-dG) large differences are seen between NLs and deoxynucleosides (Fig. 2 dashed vs solid lines). In NaCl solutions, the diC16-3'-dC CD band at 266nm exhibited a substantial shift and increase compared to diC16-3'-dC prepared in water solution (dashed green vs dotted green lines). These new bands were indicative of the formation of chiral structures. It is hypothesized that in the case of well-hydrated alkali metal salts electrostatic repulsions between the negatively charged phosphate would occur, leading to the formation of low curvature aggregates. In turn, less hydrated salts would result in higher curvature assemblies due to the stronger interaction among nucleosides. In this direction, we compared the UV and the CD spectra of NLs in pure water and in pseudo-physiological conditions (NaCl: 154 mM equivalent to 0.9% w/v). Except for diC16-3'-dG and diC16-3'-dA, which were not soluble in pseudo-physiological conditions, diC16-3'-dT and diC16-3'-dC did not show any significant change in their UV spectra. Whereas, in CD spectroscopy diC16-3'-dT exhibited a slight increase in CD intensity but for diC16-3'-dC, a large increase in CD intensity was clearly observed with a red-shift to higher wavelength (Fig. 2, bottom right, dashed vs dotted line). A different type of structure resulting from intermolecular nucleobase interactions may explain this abrupt change. These results indicate that in addition to the hydrophobic effect through the dipalmitoyl double chains, inter-stacking and H-bonding between nucleobases plays a major role in stabilizing NLs aggregates. In addition, the counter ion used in these systems strongly impact on the supramolecular organizations of diC16-dT and diC16-3'-dC. Taken together, UV-vis and CD experiments show that the diC16-3'-dX series form supramolecular assemblies, which can be modulated in the presence of NaCl.

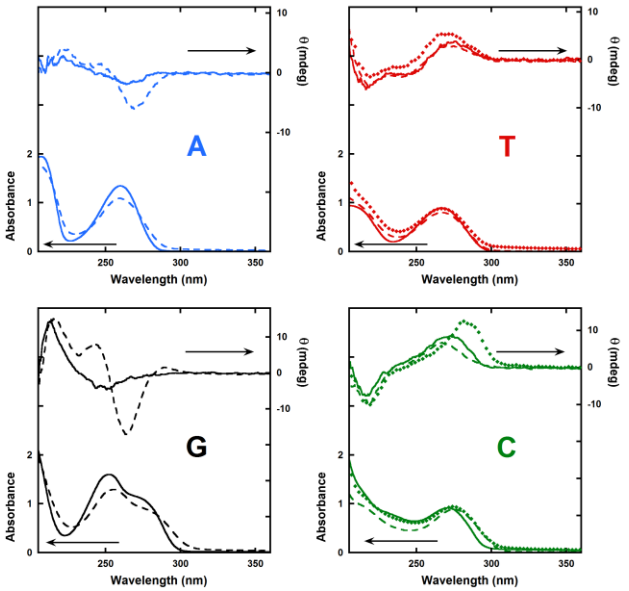

Fig. 2. UV (scale on left axis) and CD (scale on right axis) spectra of NLs prepared in water (dashed line), in 0.9% w/v NaCl solution (diamond) with their deoxynucleosides (solid line). The nature of the nucleic bases is indicated on the graphs. DiC16-3'-dG and diC16-3'-dC are not soluble in NaCl solution therefore their spectra are not displayed. All spectra were recorded at 100 µM in room temperature.

Salt effects on self-assemblies

We further investigated the supramolecular changes of NLs either in the presence or absence of NaCl. Dynamic Light Scattering (DLS) measurements were collected both in water and in NaCl conditions. The mean diameters and the polydispersity index (PDI) of the assemblies are reported as well as the size distributions graphs (Table 1 down and Figure ESI 1). In a first series of experiments, NLs were dispersed in pure water under sonication. Results obtained by DLS measurements indicated that sonication was not suitable for a good dispersion of pyrimidines NLs (diC16-3'-dC and diC16-3'-dT) giving a highly polydisperse size distribution. In contrast, for purine NLs (diC16-3'-dG and diC16-3'-dA), a single distribution was observed with a mean diameter at around 220 nm for both purine NLs with a relatively low PDI (0.23). The dispersion of NLs was also investigated in the absence of sonication. Surprisingly, in this condition, opposite behaviours are observed. Indeed, pyrimidine NLs (diC16-3'-dC and diC16-3'-dT) show a single distribution whereas purine based NLs (diC16-3'-dG and diC16-3'-dA) were not well dispersed as observed by DLS. These differences in behaviour illustrate the importance of the nucleobase in the dispersion of NLs. In NaCl conditions, size distributions of diC16-3'-dC and diC16-3'-dT (only these NLs were soluble in these conditions) showed the presence of a large size distribution with the appearance of larger structures ranging between 180 to 1000 nm, supporting the hypothesis that fibers formations occurred in the presence of well-hydrated alkali metal. The results of the DLS experiments indicated that the size of the supramolecular structures depends on the nature of the NL nucleobase. In the case of diC16-3'-dG and diC16-3-dA, bearing purine nucleobases, higher sizes of the supramolecular assemblies were observed with a tendency to form one size distribution compared with NLs possessing pyrimidine nucleobases.

Tables 1. Up) Transition temperatures by DSC of NLs obtained by DSC. The results reported are the average of four independent experiments. ± symbol indicated the standard deviation. $\Delta T_{(NaCl\ -Water)}$ emphasize the increase of transition temperatures in the presence of NaCl (0.9% w/v). Down) Z-average, diameters and polydispersity index obtained by DLS for each diC16-3'-dX.

	Transition Temperature (°C)		
	Heating Cycle		$\Delta T_{(NaCl - Water)}$
diC16-3'-dX	**Water**	**NaCl**	
diC16-3'-dA	14.2 ±0.2	38.3 ±0.4	24
diC16-3'-dT	40.0 ±3.6	41.0 ±1.5	1
diC16-3'-dG	19.8 ±0.1	40.9 ±0.8	21
diC16-3'-dC	35.4 ±0.6	41.5 ±0.8	6
	Cooling Cycle		$\Delta T_{(NaCl - Water)}$
diC16-3'-dX	**Water**	**NaCl**	
diC16-3'-dA	13.8 ±0.1	35.3 ±1.5	22
diC16-3'-dT	34.6 ±6.0	38.5 ±0.3	4
diC16-3'-dG	18.6 ±0.1	38.4 ±0.3	20
diC16-3'-dC	27.5 ±2.4	40.1 ±1.1	13

	Z-average (nm) / Particles diameters (nm)	PolyDispersity Index
diC16-3'-dX	***With sonication***	
diC16-3'-dG	186 / 238	0.232
diC16-3'-dA	199 / 220	0.234
	Without sonication	
diC16-3'-dC	99 / 105	0.089
diC16-3'-dT	81 / 85	0.193

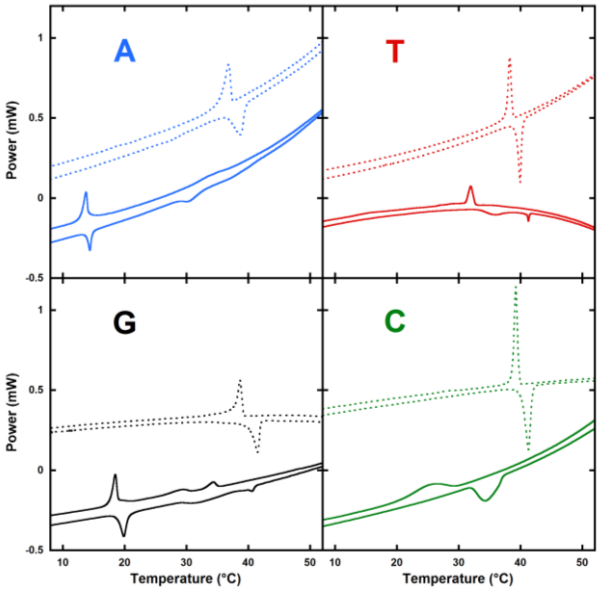

Fig. 3. DSC experiments of diC16-3'-dA (top left blue), diC16-3'-dT (top right red), diC16-3'-G (bottom left black) & diC16-3'-C (bottom right green) in the absence (solid lines) or presence of 0.9% (w/v) NaCl (dotted lines). Cooling (positive signal) and heating (negative signal) cycle are displayed. Conditions are arbitrary separated and only one cycle is shown for clarity reason.

To characterize the thermal reversibility of the hydrogels, Differential Scanning Calorimetry (DSC) experiments were performed with a total of three heating and cooling cycles in pure water and in NaCl conditions (Fig. 3). Heating and cooling cycles results from four independent runs of thermal analysis are reported in Table 1 (up).

DSC experiments showed main phases transitions (Tm) at various temperatures depending of nucleobases and conditions (Fig 3). In water, transition occurs (heating/cooling) at 15/14, 36/32, 20/19 and 35/27°C for diC16-3'-dA, diC16-3'-dT, diC16-3'-dG, and diC16-3'-dC, respectively. The Tm observed for NLs are similar to that for the natural di palmitoyl-glycerol phosphocholine (DPPC) as well as synthetic di palmitoyl uridine phosphocholine (DPUPC).[33] A clear hysteresis between heating and cooling cycle was observed for diC16-3'-dC (8°C) and diC16-3'-dT (4°C), whereas only 1°C difference occurred with diC16-3'-dG and diC16-3'-dA (See Fig 3 and Table 1 up). DiC16-3'-dG and diC16-3'-dA exhibited other small transitions. In NaCl, the main phase transition temperatures increased for all NLs and reached 39/37, 40/38, 42/39 and 42/40°C for diC16-3'-dA, diC16-3'-dT, diC16-3'-dG, and diC16-3'-dC, respectively without any additional peaks. Interestingly, a lower hysteresis between heating and cooling cycle was observed with diC16-3'-dC and diC16-3'-dT (1°C) in NaCl conditions. Note that for diC16-3'-dC and diC16-3'-dT in water, broad peaks in heating and cooling cycle were detected; this tendency did not appear in NaCl conditions. In

water condition, purine NLs (diC16-3'dT & diC16-3'-dC) showed a transition around 30°C whereas pyrimidine NLs (diC16-3'-dA & diC16-3'dG) exhibited a transition below 20°C. This main phase transition disparity between nucleobases (purine-pyrimidine) disappeared in NaCl conditions where all NLs reached approximately the same thermal reversibility at around 40°C. This observation indicates that the counter ion (Na^+) possess a stronger impact on the melting temperature of purine derivatives (diC16-3'-dA and diC16-3'-dG) than pyrimidine analogues (diC16-3'-dC and diC16-3'-dT). Although purines bases were able to give hydrogen bonding, in water condition, we observed that the transition temperatures of diC16-3'-dA and diC16-3'-dG were dramatically lower than pyrimidine NLs. This could be explained by a higher steric hindrance with purine NLs causing difficulties to self-organise. In the presence of a well-hydrated cation (Na^+), more stable assemblies could be reached suggesting that Na^+ would stabilize the supramolecular structure.

Rheology and gel behaviors

In order to further characterize the physicochemical properties of NLs at a macroscopic level, we performed gel formation experiments (Fig. 1B). Depending of the conditions (water or NaCl), striking differences were observed. In presence of NaCl, a strong diC16-3'-dC gel was formed (Fig. 1B left), whereas diC16-3'-dG precipitated without forming any gels. Following these qualitative tests, the mechanical properties of new cytidine and guanosine nucleotide-lipids based gels were analyzed using oscillatory rheology to characterize the Linear Visco-Elastic Regime (LVER) and the strength of the gels. Figure 4 shows the oscillatory strain sweeps for cytidine and guanosine nucleotide-lipids based gels at 5% and 10%, respectively. The LVER, in which the moduli are independent of the applied strain, of the new compounds were determined up to 100%. For all hydrogels investigated, the elastic G' consistently exceeds the viscous G" moduli, indicating the dominant elastic character of the nucleotide-lipid based Low Molecular Weight Gelators (LMWGs). In the case of diC16-3'-dC gels, the LVER was determined either in the absence or presence of NaCl (0.9% w/v). The breaking points measured by moduli inversion were found at 1 and 5% and the G' moduli of 600 Pa and 2400 Pa, respectively, indicating that the presence of NaCl strongly impacts on the diC16-3'-dC gels rheological properties. For diC16-3'-dG, due to the lack of solubility in the presence of NaCl, the LVER was determined only in water at 10%. At this concentration, the G derivative shows similar properties to the diC16-3'-dC at 5% in water (G'= 800 Pa, moduli inversion at 5%).

For diC16-3'-dT and diC16-3'-dC in NaCl conditions, the gel-sol transition occurred instantaneously. Note that in pure water an interstate transition between the gel to solution was observed. This gel-solution transition difference was consistent with DSC results where broad peaks were observed in water conditions contrary to sharps peaks obtained in NaCl conditions (Fig. 3, right panels). Such behaviour could explain the broad peaks obtained in heating and cooling and the large

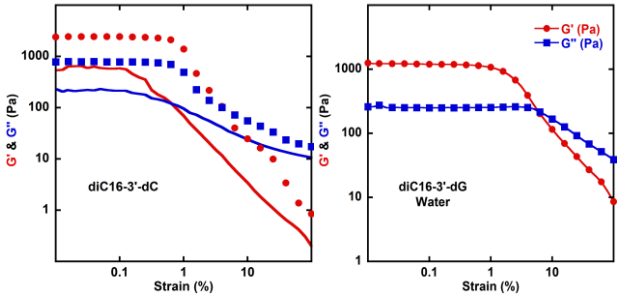

Fig. 4. Oscillatory strain sweeps for cytidine and guanosine nucleotide-lipids based gels at 5% and 10%, respectively. Elastic, (G', red) and viscous (G", blue) moduli versus strain in percent. Left) LVER of diC16-3'-dC (5%, w/v) in water (solid lines) or with 0.9% NaCl (symbols). Right) LVER of diC16-3'-dG (10%, w/v) in water

hysteresis obtained for diC16-3'-dC and diC16-3'-dT in pure water. These results also indicated that the phase transition behaviour depends mainly on the nucleobases type, the self-binding affinity between nucleobases and the environmental conditions, notably, the counter ion used.

Drug release experiments

Due to their unique properties, supramolecular gels are currently under investigation as drug delivery matrix. Controlling the kinetics of drug release from such soft materials *via* the molecular structure of gelators is highly desirable since it would allow for a modulation of drug release depending on the external conditions. To illustrate the usefulness of the novel nucleolipids in this field, in-vitro drug diffusion studies were carried out using diazepam as a drug. Diazepam is a hydrophobic compound belonging to the benzodiazepine family, which are used as an anticonvulsant in the treatment of epilepsy. The data of percentage drug release are shown in Fig. 5. For the kinetic study following plots were made: cumulative % drug release versus time for both diC16-3'-dC and diC16-3'-dG in the presence or absence of NaCl. As a general comment, a slower release is observed for both nucleolipids in the absence of NaCl ($T_{1/2}$ > 400 minutes for both compounds). After addition of NaCl, a faster release of diazepam was observed for diC16-3'-dG ($T_{1/2}$ = 20 min) compared to diC16-3'-dC ($T_{1/2}$ = 400 min), indicating that the nature of the base is playing a major role in the release mechanism from the supramolecular gels. Interestingly, these results demonstrate that the kinetic of the drug release can be modulated *via* both the nature of the base and the presence of salts.

Conclusion

In summary, a facile route for the synthesis of nucleoside-3'-monophosphate featuring the four natural nucleobases has been reported. Similarly, to thymidine and adenosine 3'-nucleotide lipids previously published, both Cytosine and Guanosine derivatives reported in this contribution exhibit self-assembly properties. Taking together, the physico-

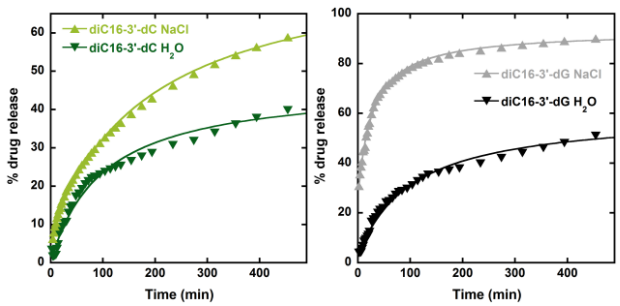

Fig. 5. In vitro drug release experiments showing the cumulative release of diazepam from the gel (% drug release) versus time (in minutes). Kinetics of release for diC16-3'-dC (left) and diC16-3'-dG (right) with the addition of water or sodium chloride solution (NaCl 0.9% w/v).

chemical studies indicate that the self-assembly properties depend strongly on both the conditions and the nature of nucleobases. The presence of NaCl induced NLs-NLs interactions, but the specific supramolecular structures achieved give rise to different states at the macrocopic level depending on the nucleobase. The control of the lipid self-assemblies *via* the molecular code of the four natural nucleotides represent a powerful strategy, which could be used to construct biocompatible soft materials such as gels. As illustrated with the drug release experiments the kinetic of release can be controlled by both the nature of the nucleobase and the presence of salts. Their nucleic acid controlled self-assembly is likely to greatly extend the potential of lipid-based materials for biomedical applications, including drug delivery.

Experimental Section

General Procedures for synthesis

All the compounds were purchased from Sigma-Aldrich, Fluka and Alfa Aesar unless otherwise mentioned. Solvents for reactions were purchased from Sigma-Aldrich in the highest quality and from VWR for other uses. All the reactions were run under nitrogen atmosphere unless otherwise stated. Analytical thin layer chromatography (TLC) was performed on pre-coated silica gel F254 plates with fluorescent indicator from Merck. The detection of compounds was accomplished using a UV light (254 nm) and visualized on TLC plates by subrsequent spraying with 10 % conc. H_2SO_4 solution in ethanol, followed by heating. Column chromatography was performed with flash silica gel (0.04-0.063 mm) from Merck. All the compounds were characterized using ^{1}H, ^{13}C and ^{31}P Nuclear Magnetic Resonance (NMR) spectroscopy. These NMR spectra were recorded (either in $CDCl_3$ obtained from Eurisotop) on BRUKER Avance DPX-300 (^{1}H at 300 MHz, ^{13}C at 75 MHz) and DPX-500 spectrometers (^{1}H at 500 MHz, ^{13}C at 125 MHz and ^{31}P at 121.49 MHz). The chemical shifts (δ) are given in parts per million (ppm) relatively residual solvent peaks ($CHCl_3$: ^{1}H: 7.26, ^{13}C: 77.16). The coupling constants J are given in Hertz (Hz); the peak multiplicity is reported as The coupling constants J are given in Hertz (Hz); the peak multiplicity is reported as follows: s = singlet, brs = broad singlet, d = doublet, t = triplet, m = multiplet. High resolution electronspray ionization mass spectra (HR ESI-MS) were performed by the CESAMO (Bordeaux, France) on a QSsat Elite mass spectrometer (applied Biosystems). The instrument is equipped with an ESI source and spectra were recorded in negative mode. The electrospray needle was maintained at 4500 V and operated at room temperature. Samples were introduced by introduced by injection through a 10 µL sample loop into a 200 µL/min flow of methanol from the LC pump. For more details, see ESI.

Preparation mode of diC16-3'-dX

DiC16-3'-dA, diC16-3'-dT, diC16-3'-dC, diC16-3'-dG were synthesized by our laboratory (see details in ESI). The simple procedure was followed for all compounds. Generic name of diC16-dX is given to specificity either DiC16-3'-dA, diC16-3'-dT, diC16-3'-dC or diC16-3'-dG. Exact mass around 6 mg of diC16-dX was weighted on 0.1 mg precision balance and dissolved and mixed in dichloromethane into 10mL volumetric flask. Aliquots were then prepared by transferring 500µL into glass vial. Aliquots were then evaporated until dryness and stored at -20°C. Hydration of the lipid film is accomplished simply by adding 3 mL mΩ water or 3mL of a NaCl solution (0.9% w/v; 154mM) The obtained solutions were then heated for 30 minutes and sonicate for 5 min at temperature of 60°C. Finally, the resulting solutions were directly assessed by either Dynamic Light Scattering, CD or UV-Vis Spectroscopy.

CD / UV-Vis Spectroscopy

UV-Vis and CD spectra of diC16-3'-dX was performed on JASCO J-1500 Circular Dichroism (optical path length=1cm) in quartz cuvette coupled with a Peltier device. All measurements were carry out at 25°C.

Differential Scanning Calorimetry

Differential Scanning Calorimetry (DSC) was realized using METTLER TOLEDO. A total of three heating and cooling cycles (5-65°C) on 2% w/w in pure water and in NaCl conditions at a constant rate of 0.5°C min^{-1} and 100µL aluminium crucible. Heating and cooling results of thermal analysis are reported in Table 1.

Dynamic Light Scattering

Dynamic Light Scattering (DLS) measurements were performed using Zetasizer 3000 HAS MALVERN at 25°C with 400 µL of a solution containing 100 µM of diC16dX prepared as explained above. Measurements of Table 1 down have been performed in water with 5 minutes sonication for purine nucleolipids (diC16-3'-dG and diC16-3'-dA) and without sonication for pyrimidines nucleolipids (diC16-3'-dC and diC16-3'-dT).

Gel Formation

Water or a NaCl solution (0.9% w/v ;154mM) were added to diC16-3'-dC or diC16-3'-dG to obtain a solution at 2% w/v of diC16-3'-dX. Then the solution was heated at 60°C during 30 minutes and sonicate the 5 last minutes. The solutions were allowed to cool down at room temperature and gel formation were observed

(diC16-3'-dC water / NaCl & diC16-3'-dG / water) or not (diC16-3'-dG NaCl). See Figure 1B.

Drug release experiments

6.0 mg of either diC16-3'-dG and diC16-3'-dC were accurately weighted in 3 mL UV cuvette. 200 µL of diazepam solution at 500 µM are added in the cuvette. Cuvette is sealed and heated at 60°C for 30 min then to cool down at room temperature for 30 min. Appearance of gel is visually checked as solution become opalescent and viscous. Cuvette is set in a Jasco V630 spectrophotometer and UV spectra (400 nm to 200 nm) is recorded every 2 min after careful addition (without disturbing the gel at the bottom of the cuvette) of 1600 µL of either water or 154 mM NaCl solution. In this setting, the beam of the spectrophotometer pass thought the bulk (above the gel) allowing to follow the kinetic of diazepam release. Absorbance at 313 nm (specific for diazepam, epsilon = 1700 $cm^{-1}.M^{-1}$) was subtracted from baseline at 350 nm and converted into percentage.

Rheology experiments

Rheological measurements were carried out on a Malvern Kinexus Pro+ rheometer with steel coneplate geometry (diameter: 40mm, angle: 1°). The lower plate is equipped with a Peltier temperature control system, and all samples were studied at 25 ± 0.01°C unless indicated otherwise. A solvent trap was used to ensure homogeneous temperature and to prevent water evaporation. The hydrogels were heated at 65°C and the resulting liquid was placed into the rheometer and subjected to sinusoidal oscillations. The experimental conditions to determine the linear visco elastic regime (LVER) were determined by performing an amplitude strain sweep from 0.01 to 100% at an angular frequency of 1Hz (6.283$rad.s^{-1}$).

Conflicts of interest and acknowledgments

There are no conflicts to declare. This work was realized under the frame of the Laboratory of Excellence AMADEus with the reference ANR-10-LABX-0042-AMADEUS, operated by the "Agence Nationale de la Recherche" under the program "Initiative for Excellence IdEx Bordeaux" (ANR-10-IDEX-0003-02). The work was also supported by INSERM and CNRS. Aurore Beaurepaire, Candice Delcourt, Alexandra Gaubert are gratefully acknowledged for their help with circular dichroism, UV-vis and rheology experiments, respectively. The authors thank the BIC Center for technical assistance during TEM observations and Marc Biran from the CRMSB.

Notes and references

1 S. Zhang, *Nat. Biotechnol.*, 2003, **21**, 1171-1178.
2 K. S. Moon, H. J. Kim, E. Lee and M. Lee, *Angew. Chem. Int. Ed.*, 2007, **46**, 6807-6810.
3 S. C. Lange, J. Unsleber, P. Drucker, H. J. Galla, M. P. Waller and B. J. Ravoo, *Org. Biomol. Chem.*, 2015, **13**, 561-569.
4 G. M. Peters and J. T. Davis, *Chem. Soc. Rev*., 2016, **45**, 3188-3206.
5 Delin Pan, Jing Sun, Hongwei Jin, Yating Li, Liyu Li, Yun Wu, Lihe Zhang and Zhenjun Yang, *Chem. Commun*., 2015, **51**, 469-472.
6 Nuthanakanti A, Srivatsan SG. *ACS Appl Mater Interfaces,* 2017, **9**, 22864–22874.
7 A. Nuthanakanti, S.G. Srivatsan, *Nanoscale,* 2016, **8**, 3607-3619.
8 A. Patwa, J. Labille, JY. Bottero, A. Thiéry, and P. Barthélémy, *Chem. Commun.,* 2015, **51**, 2547-2550.
9 J. A. Kaplan, P. Barthélémy and M. W. Grinstaff, *Chem. Commun.*, 2016, **52**, 5860-5863.
10 P. Barthélémy, C. A. H. Prata, S. F. Filocamo, C. E. Immoos, B. W. Maynor, S. A. N. Hashmi, S. J. Lee and M. W. Grinstaff, *Chem. Commun*., 2005, 1261-1263.
11 N. Rana, S. Huang, P. Patel, U. Samuni, D. Sabatino, *Bioorg Med Chem Lett.* 2016, **26**, 3567-3571.
12 C. Riccardi, D. Musumeci, C. Irace, L. Paduano, and D. Montesarchio, *Eur. J. Org. Chem.* 2017, **7**, 1100–1119.
13 C. Knies, K. Hammerbacher, G.A. Bonaterra, R. Kinscherf and H. Rosemeyer*, ChemistryOpen* 2016, **5**, 129 – 141
14 L. Latxague, M. A. Ramin, A. Appavoo, P. Berto, M. Maisani, C. Ehret, O. Chassande and P. Barthélémy, *Angew. Chem. Int. Ed.*, 2015, **54**, 4517-4521.
15 H. Rosemeyer, *Chem. Biodiv.*, 2005, **2**, 977–1062.
16 A. Gissot, M. Camplo, M. W. Grinstaff and P. Barthélémy, *Org. Biomol. Chem.*, 2008, **6**, 1324-1333.
17 J. Baillet, V. Desvergnes, A. Hamoud, L. Latxague, P. Barthélémy, *Adv. Mater.* 2018, **30** DOI: 10.1002/adma.201705078.
18 M.Y. Arteta , D. Berti, C. Montis, R.A. Campbell, C. Eriksson, L.A. Clifton , M.W. Skoda , O. Soltwedel, A. Koutsioubas, P. Baglioni, T. Nylander. *Soft Matter.* 2015, **11**, 1973-1990.
19 C. Montis, Y. Gerelli, G. Fragneto, T. Nylander, P. Baglioni, D. Berti, *Colloids Surf B Biointerfaces,* 2016, **137**, 203-213.
20 K. Sugiyasu, M. Numata, N. Fujita, S. M. Park, Y. J. Yun, B. H. Kim and S. Shinkai, *Chem. Commun.*, 2004, 1996-1997.
21 B. Desbat, N. Arazam, S. Khiati, G. Tonelli, W. Neri, P. Barthélémy and L. Navailles, *Langmuir*, 2012, **28**, 6816–6825.
22 A. Patwa, G. Salgado, F. Dole, L. Navailles and P. Barthélémy *Org. Biomol. Chem*., 2013, **11**, 7108
23 M. A. Ramin, K. R. Sindhu, A. Appavoo, K. Oumzil, M. W. Grinstaff, O. Chassande, P. Barthélémy, *Adv. Mater.*, 2017, 29, 1605227.
24 A. N. Patwa, R. G. Gonnade, V. A. Kumar, M. M. Bhadbhade, K. N. Ganesh, *J. Org. Chem.* 2010, **75**, 8705-8708.
25 J. Kumar, C. S. Purohit, S. Verma, *Chem. Commun*. 2008, **22**, 2526–2528.
26 S. Lena, S. Masiero, S. Pieraccini, GP. Spada, *Chemistry* 2009, **15**(32), 7792-806
27 L. Simeone, G. Mangiapia, C. Irace, A. Di Pascale, A. Colonna, O. Ortona, L. De Napoli, D. Montesarchio, L. Paduano, *Mol Biosyst.* 2011, **7**(11), 3075-86.
28 L. Simeone, D. Milano, L. De Napoli, C. Irace, A. Di Pascale, M. Boccalon, P. Tecilla, D. Montesarchio, *Chemistry* 2011, **17**(49):13854-65
29 D. Berti, P. L. Luisi, P. Baglioni, *Colloids Surf. A* 2000**, 167**, 95-103.
30 A. Patwa, G. Salgado, F. Dole, L. Navailles and P. Barthélémy *Org. Biomol. Chem*., 2013, **11**, 7108 .
31 S. Khiati, N. Pierre, S. Andriamanarivo, M. W. Grinstaff, N. Arazam, F. Nallet, L. Navailles and P. Barthélémy, *Bioconjugate Chem*., 2009, **20**, 1765**–**1772.
32 B. Desbat, N. Arazam, S. Khiati, G. Tonelli, W. Neri, P. Barthélémy and L. Navailles, *Langmuir*, 2012, **28**, 6816–6825.
33 L. Moreau, P. Barthélémy, Mohamed El Maataoui, and Mark W. Grinstaff *J. Am. Chem. Soc.,* 2004, **126**, 7533-7539